11-2011

Zap1 Control of Cell-Cell Signaling in *Candida albicans* Biofilms

Shantanu Ganguly
Carnegie Mellon University

Andrew C. Bishop
Duquesne University

Wenjie Xu
Carnegie Mellon University

Suman Ghosh
University of Nebraska - Lincoln

Kenneth W. Nickerson
University of Nebraska - Lincoln, knickerson1@unl.edu

See next page for additional authors

EUKARYOTIC CELL, Nov. 2011, p. 1448–1454 Vol. 10, No. 11
1535-9778/11/$12.00 doi:10.1128/EC.05196-11

Zap1 Control of Cell-Cell Signaling in *Candida albicans* Biofilms▽†

Shantanu Ganguly,[1] Andrew C. Bishop,[2] Wenjie Xu,[1] Suman Ghosh,[3] Kenneth W. Nickerson,[3] Frederick Lanni,[1] Jana Patton-Vogt,[2] and Aaron P. Mitchell[1]*

Department of Biological Sciences, Carnegie Mellon University, Pittsburgh, Pennsylvania 15213[1]; Department of Biological Sciences, Duquesne University, Pittsburgh, Pennsylvania 15282[2]; and School of Biological Sciences, University of Nebraska, Lincoln, Nebraska 68588-0666[3]

Received 4 August 2011/Accepted 25 August 2011

Biofilms of *Candida albicans* include both yeast cells and hyphae. Prior studies indicated that a *zap1*Δ/Δ mutant, defective in zinc regulator Zap1, has increased accumulation of yeast cells in biofilms. This altered yeast-hypha balance may arise from internal regulatory alterations or from an effect on the production of diffusible quorum-sensing (QS) molecules. Here, we develop biosensor reporter strains that express yeast-specific *YWP1-RFP* or hypha-specific *HWP1-RFP*, along with a constitutive *TDH3-GFP* normalization standard. Seeding these biosensor strains into biofilms allows a biological activity assay of the surrounding biofilm milieu. A *zap1*Δ/Δ biofilm induces the yeast-specific *YWP1-RFP* reporter in a wild-type biosensor strain, as determined by both quantitative reverse transcription-PCR (qRT-PCR) gene expression measurements and confocal microscopy. Remediation of the *zap1*Δ/Δ zinc uptake defect through zinc transporter gene *ZRT2* overexpression reverses induction of the yeast-specific *YWP1-RFP* reporter. Gas chromatography-mass spectrometry (GC-MS) measurements of known organic QS molecules show that the *zap1*Δ/Δ mutant accumulates significantly less farnesol than wild-type or complemented strains and that *ZRT2* overexpression does not affect farnesol accumulation. Farnesol is a well-characterized inhibitor of hypha formation; hence, a reduction in farnesol levels in *zap1*Δ/Δ biofilms is unexpected. Our findings argue that a Zap1- and zinc-dependent signal affects the yeast-hypha balance and that it is operative in the low-farnesol environment of the *zap1*Δ/Δ biofilm. In addition, our results indicate that Zap1 is a positive regulator of farnesol accumulation.

Biofilms are complex microbial communities embedded in a matrix layer (10). Biofilm cells exhibit unique phenotypes compared to free-living planktonic cells (10). Microbial biofilms are common in nature and are a leading cause of human infection (11, 15). Therefore, it is important to identify the mechanisms that govern biofilm formation to better understand microbial ecology and disease.

Quorum-sensing (QS) molecules are extracellular metabolites that relay information about cell density and affect cell physiology (18, 25). These molecules assume vital importance in multicellular structures like biofilms. QS molecules were first identified in bacteria but are also found in eukaryotic microbes, such as *Candida albicans*, a major fungal pathogen and the focus of our study. Several QS molecules have been shown to affect cell physiology in *C. albicans* (18, 25). The roles of these molecules have been studied both with planktonic cells (4, 5, 13, 20) and in the context of biofilms (23, 28).

The accumulation and distribution of QS molecules in *C. albicans* biofilms play important roles in biofilm development. For example, the first discovered *C. albicans* QS molecule, farnesol, functions as an inhibitor of the transition from ovoid yeast cells to filamentous hyphal cells (4, 5, 13, 20). As yeast cells are less adherent than hyphal cells, it is believed that production of yeast cells in a mature biofilm, promoted by farnesol accumulation, leads to dispersal of the biofilm. Ultimately, dispersal *in vivo* leads to disseminated infection. Yeast cells released from a biofilm have novel properties, including increased virulence and drug tolerance, that augment the severity of biofilm-based *C. albicans* infections (10, 32).

Our study addresses the role of a *C. albicans* transcription factor, Zap1 (*z*inc-responsive *a*ctivator *p*rotein; also called Csr1), which governs the balance of yeast and hyphal cells in biofilms. Zap1 has been identified as a regulator that is required for efficient hypha formation (22). It has considerable homology to the *Saccharomyces cerevisiae* zinc regulator ScZap1 (9, 34), and indeed, it also controls the expression of zinc transporters and other zinc-regulated genes (22, 27). Our interest in Zap1 is based on its role in biofilm structure: *zap1*Δ/Δ mutant biofilms produce excess β-glucan, a component of the extracellular matrix, and also have increased accumulation of yeast cells (27). Direct Zap1 target genes, identified by chromatin immunoprecipitation, do not include known yeast- or hypha-specific genes (27), so the relationship between Zap1 and cellular morphogenesis seems indirect. Here, we provide evidence that Zap1 governs the accumulation of farnesol in biofilms. In addition, findings point to uptake of zinc itself as a determinant of cell-cell signaling.

MATERIALS AND METHODS

Media. *C. albicans* strains were grown at 30°C in YPD (2% glucose, 2% Bacto-peptone, 1% Bacto-yeast extract) for Ura$^+$ strains or YPD plus Uri (2% glucose, 2% Bacto-peptone, 1% Bacto-yeast extract, 80 μg/μl of uridine) for Ura$^-$ strains. Transformants were selected on complete supplemental medium (CSM) (MP Biomedicals, LLC) plates containing 2% glucose, 0.67% yeast nitrogen base (without amino acids), 2% Bacto-agar, and one of the following dropout media: CSM-URA, CSM-ARG-URA, or CSM-HIS (MP Biomedicals, LLC). Biofilms were grown in spider medium (10 g D-mannitol [Sigma], 10 g

* Corresponding author. Mailing address: Department of Biological Sciences, Carnegie Mellon University, Pittsburgh, PA 15213. Phone: (412) 268-5844. Fax: (412) 268-7129. E-mail: apm1@cmu.edu.

† Supplemental material for this article may be found at http://ec.asm.org.

▽ Published ahead of print on 2 September 2011.

TABLE 1. Yeast strains

Strain	Genotype	Reference
BWP17	*ura3*Δ::λ*imm434 arg4*::*hisG his1*::*hisG* *ura3*Δ::λ*imm434 arg4*::*hisG his1*::*hisG*	33
DAY185	*ura3*Δ::λ*imm434 ARG4*:*URA3*::*arg4*::*hisG his1*::*hisG*::*pHIS1* *ura3*Δ::λ*imm434 arg4*::*hisG his1*::*hisG*	7
CJN1201	*ura3*Δ::λ*imm434 arg4*::*hisG his1*::*hisG*::*pHIS1 zap1*::*ARG4* *ura3*Δ::λ*imm434 arg4*::*hisG his1*::*hisG zap1*::*URA3*	27
CJN1651	*ura3*Δ::λ*imm434 arg4*::*hisG his1*::*hisG*::*pHIS1 zap1*::*ARG4 ZRT1*::*pAgTEF1-NAT1-AgTEF1UTR-TDH3-ZRT1* *ura3*Δ::λ*imm434 arg4*::*hisG his1*::*hisG zap1*::*URA3 ZRT1*	27
CJN1655	*ura3*Δ::λ*imm434 arg4*::*hisG his1*::*hisG*::*pHIS1 zap1*::*ARG4 ZRT2*::*pAgTEF1-NAT1-AgTEF1UTR-TDH3-ZRT2* *ura3*Δ::λ*imm434 arg4*::*hisG his1*::*hisG zap1*::*URA3 ZRT2*	27
CJN1193	*ura3*Δ::λ*imm434 arg4*::*hisG his1*::*hisG*::*pHIS1-ZAP1 zap1*::*ARG4* *ura3*Δ::λ*imm434 arg4*::*hisG his1*::*hisG zap1*::*URA3*	27
SGH281	*ura3*Δ::λ*imm434 ARG4 his1*::*hisG*::*pHIS1-pTDH3-GFP-tADH1 YWP1*::*pYWP1-RFP-tADH1-URA3* *ura3*Δ::λ*imm434 arg4*::*hisG his1*::*hisG YWP1*	This study
SGH284	*ura3*Δ::λ*imm434 ARG4 his1*::*hisG*::*pHIS1-pTDH3-GFP-tADH1 HWP1*::*pHWP1-RFP-tADH1-URA3* *ura3*Δ::λ*imm434 arg4*::*hisG his1*::*hisG HWP1*	This study

nutrient broth [BD Difco]), 2 g K_2HPO_4 [Sigma] in 1 liter of distilled water) at 37°C.

Plasmid and strain construction. The reference (DAY185), *zap1*Δ/Δ (CJN1201), and *zap1*Δ/Δ/+ (CJN1193) strains used in the study have been previously described (7, 27). In addition, the *ZRT1*- and *ZRT2*-overexpressing strains CJN1651 and CJN1655 have been previously described (27). Newly constructed *C. albicans* reporter strains (Table 1) were derived from BWP17 (33). All primer sequences are listed in Table S5 in the supplemental material. The strain BWP17 was made Arg^+ by addition of *ARG4* at the native locus by transformation with the PCR product of primers SG272 and SG273. The strain SGH275, which contained *RFP* downstream of the *YWP1* promoter, was designed by amplifying an *RFP-URA3* cassette from plasmid pMG2169 (12), using primers SG238 and SG239, and transforming the PCR product into the Arg^+ BWP17 derivative to target the cassette at the *YWP1* locus. Similarly, strain SGH278, which contained *RFP* downstream of the *HWP1* promoter, was designed by amplifying an *RFP-URA3* cassette from plasmid pMG2169, using primers SG236 and SG237, and transforming the PCR product into BWP17 to target the cassette at the *HWP1* locus. For construction of the normalization construct, plasmid pSG36 was used. The plasmid was created by *in vivo* recombination in *S. cerevisiae* strain BY4741 Δ*trp* (3) by using the following sequences bearing regions of homology to each other: the PCR product of primers SG232 and SG233 (which amplify the *TDH3* promoter from *C. albicans* reference strain genomic DNA), the PCR product of primers SG234 and SG235 (which amplify *GFP-*T_{ADH1} from pJRB103), and NotI-digested pDDB78 (2, 30). This plasmid was integrated at the *HIS1* locus by digesting it with NruI and transforming it into both strains SGH275 and SGH278 to yield the yeast cell reporter strain (SGH281) and hyphal cell reporter strain (SGH284), respectively.

Quantification of excreted alcohols in biofilm supernatants. For quantification of alcohols in biofilm supernatants, cells were grown as biofilms in 50 ml of spider medium in 150-cm^2 tissue culture flasks (Corning flask, tissue culture treated; catalog number 430823) in order to maximize the surface area of biofilm growth and permit detection of alcohols of the biofilm supernatants after sample processing. Cells from overnight cultures of DAY185, CJN1201, and CJN1193 in YPD were added to each flask at a final optical density at 600 nm (OD_{600}) of 0.5 in 50 ml spider medium. Cell adherence was done for 90 min at 37°C with 35 rpm agitation in the incubator. After the cell adherence step, the flasks were washed with phosphate-buffered saline (PBS), and 50 ml of fresh spider medium was added to the flasks. Biofilms were grown for 48 h at 37°C with 35 rpm agitation. Biofilm supernatants were collected by first disrupting the biofilms formed on the bottoms of the flasks using a cell scraper, followed by pipetting to ensure removal of adherent cells. Following mechanical disruption of the biofilms, the samples were transferred to 50-ml plastic tubes and centrifuged at 5,000 rpm for 10 min to pellet all the cells. The supernatants were then vacuum filtered to ensure removal of all cellular debris and stored at −80°C until samples were processed for gas chromatography-mass spectrometry (GC-MS). The cell debris was resuspended in distilled water and vacuum filtered to be used for dry-weight estimation. Filters with vacuum-filtered cell pellets for each sample were allowed to bench dry in petri dishes and weighed regularly to calculate the biofilm dry weight. The final biofilm dry weights were determined by subtracting the weight of the filter before from the weight after collection of the biofilm cell pellet for each sample.

Extraction and GC-MS analysis of secreted farnesol, phenethyl alcohol, tyrosol, and tryptophol were performed by modification of a previously described method (13). Briefly, 50 ml of 48-hour biofilm medium depleted of cells was extracted with 20 ml of ethyl acetate (E196-4; Fisher Scientific) by vigorous mixing in a separatory funnel. The ethyl acetate (top) phase was concentrated using rotary evaporation. Samples were suspended in 2 ml of ethyl acetate and filtered through 0.2-μm nylon membrane filters (Whatman 7402-001) into GC vials. One microliter of each sample was injected into a Varian CP-3800 gas chromatograph in tandem with a Varian Saturn 2000 mass spectrometer (GC-MS). Varian FactorFour VF-5ms 30-m (CP8944) or 60-m (CP8960) capillary columns were used. The MS was in electron ionization (EI) mode, scanning from a range of 40 to 350 mass-to-charge ratio. The transfer line temperature was set to 280°C, and the trap temperature was set to 200°C. The following standards were used for identification and quantification of peaks: farnesol, Alfa Aesar A19316; tryptophol, Alfa Aesar 526-55-6; tyrosol, Maybridge SB01196DE; and phenethyl alcohol, Acros Organics 130180050.

For the 30-m column, the flow rate was 1.0 ml/min, and the inlet temperature was set to 280°C. The temperature program was 80°C held for 2 min, followed by a 60°C/min increase to 160°C, which was held for another 2 min. Finally, there was a 10°C/min increase in temperature until 300°C was reached, followed by a 5-min hold. The total run time was 24.33 min, and a 5-min solvent delay was used for the MS.

For the 60-m column, the flow rate was 1.5 ml/min, and the inlet temperature was set to 280°C. The temperature program was 80°C held for 2 min, followed by a 60°C/min increase to 160°C, which was held for another 2 min. Finally, there was a 15°C/min increase in temperature until 300°C was reached, followed by a 5-min hold. The total run time was 19.67 min, and a 6-min solvent delay was used for the MS.

Individual peak areas were identified from the GC-MS spectra based on the positions of the standards in the spectra. The peak area and known standard concentration value for each alcohol on the mass spectra were used to calculate the amounts of alcohol extracted from the biofilm supernatant. The efficiency of this ethyl acetate extraction was measured by performing the extraction on known concentrations of the alcohols in spider medium. The approximate percent recoveries for the alcohols were as follows: tyrosol, 33% ± 7%; farnesol,

35% ± 13%; phenethyl alcohol, 50% ± 16%; and tryptophol, 86% ± 4%. Estimates from three independent biological experiments were divided by the biofilm dry weight for each experiment, and the average and standard deviation were calculated.

RNA extraction from biofilms. RNA extraction from biofilms was carried out using a modification of a previously described protocol (27). Biofilms for gene expression analysis by quantitative reverse transcription-PCR (qRT-PCR) were grown in six-well polystyrene plates (Costar 3736 6-well untreated plates; catalog number 07201588) that were pretreated overnight with 4 ml fetal bovine serum (FBS) (HI Sigma F4135 or Gibco HI FBS 16140) and placed in a 37°C incubator (New Brunswick Scientific; I26 and ISS) with agitation at 35 rpm. The same day, the strains of interest were grown overnight in 5 ml YPD medium. The following day, the six-well plates were washed with PBS, and 4 ml spider medium was added to each well. Cells from the overnight culture were added to each well at a final OD_{600} of 0.5. For the mixed biofilm assays, overnight cultures of DAY185, CJN1201, CJN1193, CJN1651, and CJN1655 were added to each well at a final OD_{600} of 0.4, while the reporter strain (SGH281 or SGH284) was added to each well at a final OD_{600} of 0.1. Cell adherence was done for 90 min at 37°C with 35 rpm agitation in the incubator. After the cell adherence step, the six-well plates were washed with PBS, and 4 ml of fresh spider medium was added to the wells. Biofilms were grown for 48 h at 37°C with 35 rpm agitation. The biofilms were harvested by scraping the bottoms of the six-well plates using a cell scraper and filtering the cell slurry of the all the wells in the six-well plate on a vacuum manifold. The filters were flash frozen immediately after harvesting each sample. The cells were kept frozen on filters at −80°C until RNA extraction. RNA was extracted using a RiboPure-Yeast kit (Ambion) following the manufacturer's instructions with the following modifications as described previously (2). Cells were resuspended from filters with 1.5 ml ice-cold distilled water, followed by 10 to 15 s of vigorous vortexing. The resuspended cells were transferred to a 1.5-ml tube and spun down according to the manufacturer's protocol. During the cell disruption step, the cells were beaten with a Next Advance Bullet Blender for 3 min at 4°C for cell lysis.

qRT-PCR expression analysis. The qRT-PCR analysis was carried out according to the protocol described previously (2). The extracted total RNA from the previous step (0.10 μg) was treated with a DNA-free kit (Ambion). This was followed by first-strand cDNA synthesis from half of the DNA-free RNA using the AffinityScript multiple-temperature cDNA synthesis kit (Stratagene). Absence of DNA contamination was confirmed using control sample sets to which reverse transcriptase was not added from the cDNA reaction.

Primer3 software (http://frodo.wi.mit.edu/) was used to design primers (see Table S5 in the supplemental material) for *RFP* (primers SG276 and SG277) and *GFP* (primers SG274 and SG275). The RT-PCR conditions were as follows: 2× iQ SYBR green Supermix (Bio-Rad), 1 μl of first-strand cDNA reaction mixture, and 0.1 μM primers were mixed in a total volume of 50 μl per reaction. Real-time PCR was carried out in triplicate for each sample using the iCycler iQ real-time PCR detection system (Bio-Rad). The program for amplification includes an initial denaturation step at 95°C for 5 min, followed by 40 cycles of 95°C for 45 s and 58°C for 30 s. Product amplification was detected using SYBR green fluorescence during the 58°C step. The reaction specificity was monitored by melting curve analysis. *PTDH3-GFP* was used as a reference gene for normalization of gene expression, which was done using Bio-Rad iQ5 software ($\Delta\Delta C_T$ method). For the mixed-biofilm experiments, the results shown are averages and standard deviations from three independent biological experiments.

Effects of farnesol under planktonic and biofilm conditions. The effects of farnesol on yeast and hyphal cell reporters under planktonic condition was carried by using a previously described method with the following modifications (8). Dimethyl sulfoxide (DMSO) (Fisher Scientific; D128-500) was used as a solvent (19) for making 2 M stock solutions of farnesol (Alfa Aesar A19316 and Sigma F203-25G). No difference in the biological activities of the farnesols from the two manufacturers was observed. These stocks were stored at −20°C after purging with argon, and a fresh stock solution was used each time before an experiment. Working solutions of 7.5 mM and 20 mM were made using the 2 M stock solution in water, and equivalent amounts of DMSO were used for mock treatment (final concentration, 0.1%). Both the stocks and mock treatment solutions were filter sterilized prior to addition to spider medium to achieve final concentrations of 75 μM and 200 μM. Overnight cultures of yeast and hyphal cell reporters in YPD were diluted to an initial concentration of 1×10^6 cells per ml in 25 ml of prewarmed spider medium containing 0.1% DMSO (mock) or 75 μM and 200 μM farnesol. They were allowed to grow for 2 h in a 37°C incubator (New Brunswick Scientific; I26 and ISS) with agitation at 225 rpm. After 2 h, cells were harvested by filtering on a vacuum manifold, followed by flash freezing the samples. The samples were frozen on filter papers at −80°C until RNA extraction was carried out. RNA extraction was carried out in the same way as described above. For microscopic analysis, cells from overnight cultures of yeast and hyphal cell reporter in YPD were diluted to 5×10^5 cells per ml on poly-D-lysine-coated glass bottom dishes (Mat Tek Corp.; P35GC-1.5-14-C) and were grown in spider medium containing 0.1% DMSO (mock) or 75 μM and 200 μM farnesol for 4 h at 37°C. The dishes were imaged on a Zeiss microscope using a 63× objective to assess cell morphology. For analysis of the yeast and hyphal reporter gene expression, samples were washed once with CSM and resuspended in CSM prior to imaging to minimize autofluorescence caused by spider medium under the red and green channels.

Confocal microscopy of mixed biofilms. For confocal microscopy, cells were grown on the surfaces of silicone squares using a previously described protocol (26). Briefly, silicone discs were incubated at 37°C overnight in a 12-well plate with fetal bovine serum (HI Sigma F4135 or Gibco HI FBS 16140). They were washed with 2 ml PBS, and 2 ml of spider medium was added to each well. Cells from the overnight YPD cultures were added to each well at a final OD_{600} of 0.4 for DAY185 and CJN1201 and a final OD_{600} of 0.1 for the yeast reporter strain (SGH281). Cell adherence was done for 90 min at 37°C with 60 rpm agitation in the incubator. After the cell adherence step, the 12-well plates were washed with PBS, and 2 ml of fresh spider medium was added to the wells. Biofilms were grown for 48 h at 37°C with 60 rpm agitation. After 24 h, the plates containing biofilms were removed from the incubator for fixing and processing. Each culture was drained with a fine aspirator and refilled with 3.5 ml of 4.0% formaldehyde in PBS as a fixative. Fixation was allowed to proceed on a slow orbital mixer for 4 h, after which all silicone squares were transferred to 50% glycol-methacrylate (GMA) (Electron Microscopy Sciences Inc.) in distilled water. All steps involving fixative or GMA were carried out in a fume hood or with the specimens in closed containers. Control and experimental biofilms were infiltrated in separate labeled dishes under slow orbital mixing for 40 min. The biofilms were then infiltrated overnight in 97% GMA activated with benzoyl peroxide. After 20 h, individual silicone squares were inverted onto pools of activated GMA held in circular wells formed from stacked pairs of 300-μm white silicone Swinnex gaskets (Millipore Corp.) mounted on coverglasses. This positioned each biofilm in liquid GMA with the apical side downward but suspended 100 to 300 μm away from contact with the coverglass. The mounted specimens were then deoxygenated for 3 h in a UV-transparent plastic box under flowing argon gas, after which a standard long-wave UV light box was used to initiate GMA polymerization for 30 min with continued argon flow and with air cooling to prevent heat transfer from the light box to the specimens. After 30 min, polymerization was allowed to continue for several hours under argon at ambient temperature. GMA polymer formed in this way is a transparent glassy solid with a refractive index close to 1.5, which greatly reduces the opacity of the fixed biofilms. Specimens were imaged through the coverglass in an apical-to-basal direction by serial-focus optical-sectioning fluorescence microscopy carried out using a slit-scan confocal optical unit on a Zeiss Axiovert 200 microscope. A 40× 0.85-numerical-aperture (NA) oil immersion objective (Zeiss 461707 with ICS adapter 444907) provided sufficient working distance to image to the base of all mounted biofilms. "Three-dimensional" (3D) image stacks corresponding to a 100- to 450-μm focus range in 0.86- to 1.00-μm focus increments and 0.16-μm pixilation were processed using ImageJ software (http://rsbweb.nih.gov/ij/). Separate confocal image stacks obtained for each field of view using fluorescein/green fluorescent protein (GFP) and rhodamine/Cy3/red fluorescent protein (RFP) filter sets were registered axially and transversely. The images were then converted to 32-bit format for floating-point operations. Out-of-focus fluorescence was removed from each image by subtraction of a smoothed background, and a threshold of >1 was set in both the green and red stacks to exclude background pixels. Even with the index-matching afforded by poly-GMA embedding, attenuation of fluorescence with focus depth was evident in both the green and red stacks. Therefore, to quantify RFP reporter gene expression, the ratio image stack was computed through pixel-by-pixel division of the processed "red-channel" image stack by the processed "green-channel" image stack. The resulting red/green ratio image stack was then resliced to produce a side view stack showing the axial profile from apex to base. The side view stack was then projected onto a single plane and displayed in a 16-color spectral scale in which a low red/green ratio (low reporter expression) was coded blue and a high red/green ratio (high reporter expression) was coded red/white.

RESULTS

Yeast cell and hyphal biosensor reporter strain development. Microarray data had indicated that *zap1*Δ/Δ mutant biofilms have altered levels of yeast- and hypha-specific gene RNA accumulation, in keeping with their increased numbers

of yeast cells (27). The role of Zap1 in the yeast-hypha balance might be direct; previously identified Zap1 targets may include an uncharacterized regulator of cell morphogenesis. A second model is that Zap1 governs the yeast-hypha balance indirectly through production of QS molecules. We sought to test this model by including wild-type biosensor reporter cell populations in *zap1*Δ/Δ mutant biofilms. The reporter cells would allow an assay of the response of wild-type cells to the *zap1*Δ/Δ mutant biofilm environment.

We developed the biosensor reporter strains as follows. The yeast cell reporter strain had an *RFP* coding region replacing one allele of the yeast-specific *YWP1* (*y*east form *w*all *p*rotein) gene (14, 17, 29), so that *RFP* was fused to the *YWP1* promoter and 5′ region. The hyphal reporter strain had an *RFP* coding region replacing one allele of the hypha-specific *HWP1* (*h*yphal *w*all *p*rotein) gene (17, 29, 31), so that *RFP* was fused to the *HWP1* promoter and 5′ region. Each strain also contained a copy of *GFP* fused to the constitutive *TDH3* promoter as a normalization control. Thus, we could measure the RFP/GFP ratio, through gene expression or microscopy assays, to determine relative *YWP1* or *HWP1* expression among the biosensor reporter cells. To verify the behavior of the reporter strains, we grew them under well-characterized planktonic conditions that favor yeast or hypha formation and analyzed gene expression by microscopy and quantitative RT-PCR. We observed (see Fig. S1 in the supplemental material) that the yeast cell reporter strain expressed RFP under yeast growth conditions and not hyphal growth conditions; it expressed the GFP control under both conditions. In addition, the hyphal reporter strain expressed RFP under hyphal growth conditions and not yeast growth conditions; again, GFP was expressed under both conditions. Quantitative RT-PCR assays (see Fig. S1 in the supplemental material), in which RFP RNA was normalized to GFP RNA for each strain, verified that the yeast cell reporter strain expressed RFP RNA at higher levels under yeast growth conditions than under hyphal growth conditions; the hyphal reporter strain did the opposite. The reporter strains thus behave as expected from prior studies of *YWP1* and *HWP1* expression and of *C. albicans* morphogenesis.

We characterized the response of the reporter strains to farnesol under planktonic growth conditions. Prior studies had shown that exogenous farnesol inhibits hypha formation and hypha-specific gene expression (8, 20, 25). Exogenous farnesol, at concentrations reported to suppress hypha formation (75 μM and 200 μM farnesol [8]), repressed RFP fluorescence and RNA accumulation in the hyphal reporter strain and promoted RFP fluorescence and RNA accumulation in the yeast cell reporter strain (see Fig. S2 in the supplemental material). These observations confirm that the reporter strains manifest the expected responses to farnesol.

Control of intercellular signaling in biofilms by Zap1 and Zrt2. In order to assay the role of Zap1 in intercellular biofilm signaling, we seeded reporter strains into biofilms of the *zap1*Δ/Δ mutant or the wild-type and complemented strains. The reporter strain comprised 20% of the population, a level that permitted reliable detection of reporter strain RNA. When the yeast cell reporter strain was seeded into biofilms, we observed approximately 2-fold-higher levels of *YWP1-RFP* RNA in biofilms dominated by the *zap1*Δ/Δ mutant than in the *zap1*Δ/Δ/+ complemented strain and the wild-type strain (Fig. 1). Confocal microscopy verified increased RFP expression by the reporter cells in *zap1*Δ/Δ mutant biofilm compared to the wild-type biofilm (Fig. 2; see Video S6 in the supplemental material). Phase-contrast images indicated that yeast cells were found primarily in the basal layer of the biofilm (data not shown), as described previously for this *in vitro* model (10, 16). (Fixed embedded biofilms were used for microscopy because fixed samples have a nearly uniform refractive index, reducing light scattering and thus improving light penetration through thick biofilms.) We did not observe a significant difference in *HWP1-RFP* RNA levels when the hyphal reporter strain was seeded into such biofilms (see Fig. S3 in the supplemental material), probably because of the preponderance of hyphal cells in mature biofilms. These results indicate that the *zap1*Δ/Δ biofilm environment includes signals that promote *YWP1* expression in wild-type cells.

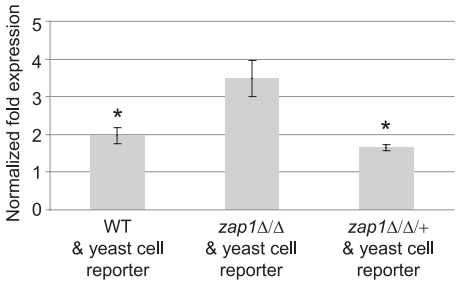

FIG. 1. Yeast cell reporter expression analysis in mixed biofilms. The mutant strain CJN1201 (*zap1*Δ/Δ), the complemented strain CJN1193 (*zap1*Δ/Δ/+), and the reference wild-type (WT) strain (*ZAP1*/*ZAP1*) were grown with SGH281 (yeast cell reporter) at a ratio of 4 to 1. Quantitative RT-PCR expression analysis of the yeast reporter was carried out on total biofilm RNA extracted from 48-h mixed biofilms. The asterisks indicate that expression levels of the yeast cell reporter were significantly lower in the mixed biofilm with *zap1*Δ/Δ/+ ($P = 0.0074$) and *ZAP1*/*ZAP1* ($P = 0.0028$) strains than in the mixed biofilm with the *zap1*Δ/Δ mutant. The error bars indicate standard deviations.

We envisioned that the loss of Zap1 has phenotypic impact for two general reasons. First, there are the direct consequences of altered Zap1-regulated gene expression. Second, there are the consequences of zinc limitation. The latter point reflects the fact that Zap1 activates the expression of two genes specifying zinc transporter homologs, *ZRT1* and *ZRT2* (*z*inc-*r*egulated *t*ransporter), and thus, a *zap1*Δ/Δ mutant grows poorly on media with low zinc levels (22). We observed previously that overexpression of *ZRT2*, but not *ZRT1*, improves the growth of the *zap1*Δ/Δ mutant on low-zinc medium (27). To test whether biofilm zinc limitation leads to an altered yeast-hypha balance, we assayed *YWP1-RFP* expression in the yeast cell reporter strain seeded into biofilms of *zap1*Δ/Δ strains that overexpress *ZRT1* or *ZRT2*. Overexpression of *ZRT2*, but not *ZRT1*, restored *YWP1-RFP* expression to levels observed in wild-type biofilms (Fig. 3). These results indicate that zinc limitation contributes to the altered yeast-hypha ratio that is induced in *zap1*Δ/Δ biofilms.

Zap1 control of farnesol accumulation. Our above observations could be explained if Zap1 is required for normal accumulation of QS molecules, such as farnesol, tyrosol, tryptophol, and phenethyl alcohol (4, 5, 13, 20). We used GC-MS analysis of biofilm supernatants (13) to test this idea. Biofilms

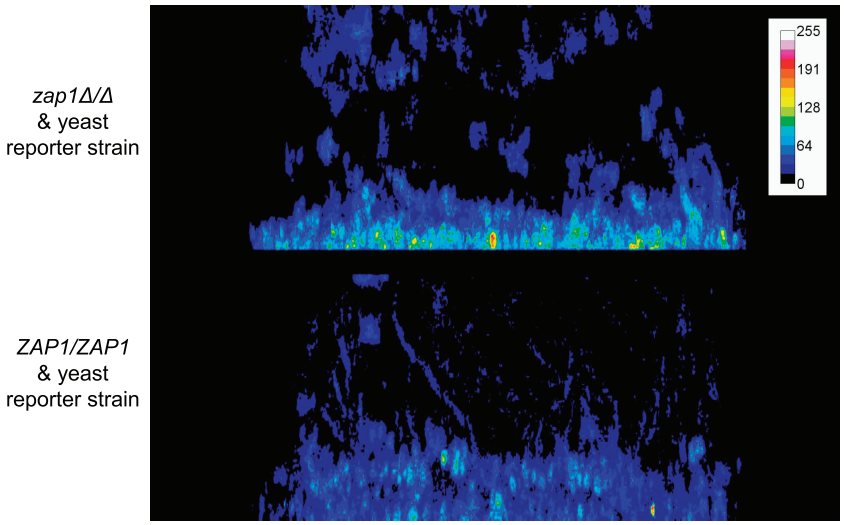

FIG. 2. Yeast cell reporter expression microscopic analysis in mixed biofilms. The mutant strain CJN1201 (*zap1*Δ/Δ mutant) and the reference wild-type strain DAY185 (*ZAP1*/*ZAP1*) were grown with SGH281 (yeast cell reporter) at a ratio of 4 to 1. Confocal microscopic expression analysis of the yeast reporter was carried out on 24-h mixed biofilms. RFP channel/GFP channel ratio images are shown. Only cells that express RFP are visible in the image, as reflected in the RFP/GFP ratio scale bar on the right.

were grown for 48 h to yield comparable biomasses (see Table S4 in the supplemental material). We observed that biofilms of the *zap1*Δ/Δ mutant strain produced less farnesol per gram of biofilm biomass than the *zap1*Δ/Δ/+ complemented strain or the wild-type strain (Fig. 4A). Similar results were obtained under planktonic growth conditions (data not shown). No significant differences in the levels of tyrosol, tryptophol, and phenethyl alcohol were observed among the mutant, complemented, and wild-type strains (Fig. 4A), though there was a trend toward lower tyrosol levels in the mutant that was not significant. These results indicate that Zap1 is a positive regulator of farnesol production.

We then tested the hypothesis that *ZRT2* overexpression in the *zap1*Δ/Δ strain may impact the yeast reporter strain response through an effect on farnesol production. GC-MS analysis of biofilm supernatants indicated that *ZRT2* overexpression did not alter the production of known QS molecules in the *zap1*Δ/Δ background (Fig. 4B). Our results indicate that diminished farnesol production results from a Zap1 regulatory defect that is independent of the *ZRT2* expression defect.

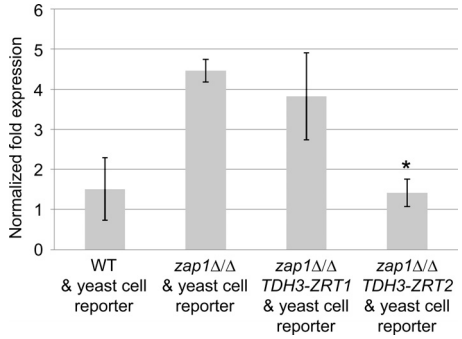

FIG. 3. *ZRT2* affects *YWP1* expression in *zap1*Δ/Δ mutant biofilm. The mutant strain CJN1201 (*zap1*Δ/Δ); the mutant strains overexpressing *ZRT1*, CJN1651 (*TDH3-ZRT1* in *zap1*Δ/Δ), and *ZRT2*, CJN1655 (*TDH3-ZRT2* in *zap1*Δ/Δ), and the reference wild-type strain, DAY185 (*ZAP1*/*ZAP1*), were grown with SGH281 (yeast cell reporter) at a ratio of 4 to 1. Quantitative RT-PCR expression analysis of the yeast reporter was carried out on total biofilm RNA extracted from 48-h mixed biofilms. The asterisk indicates that expression levels of the yeast cell reporter were significantly lower in the mixed biofilm with *zap1*Δ/Δ overexpressing *ZRT2* ($P = 0.003$) than in the *zap1*Δ/Δ mutant.

DISCUSSION

Biofilms are a significant context in which QS molecules function. In *C. albicans*, the yeast-hypha transition is a major target of QS control. Here, we have studied cell-cell signaling in biofilms formed by a *zap1*Δ/Δ mutant, which have elevated yeast form cell contents. We implemented a biosensor approach, the use of wild-type reporter cells, which revealed that the increased propensity of the *zap1*Δ/Δ mutant to form yeast cells is mediated by cell-cell signaling, as opposed to an internal cell-delimited regulatory circuit. GC-MS measurements of all known organic QS molecules yielded a surprising result: that the *zap1*Δ/Δ mutant has greatly reduced levels of farnesol, a situation that would be expected to decrease the proportion of yeast cells. Interestingly, while Zap1 is required for full production of farnesol, it appears that zinc uptake has an additional effect on cell-cell signaling, one that is mediated by an unidentified molecule (Fig. 5).

Previously published microarray analysis (27) of the *zap1*Δ/Δ mutant provides a simple explanation for its reduced levels of farnesol. The mutant has reduced expression of *DPP1*, which specifies a putative diacylglycerol pyrophosphate phosphatase. Such an activity is thought to generate farnesol from the ergosterol biosynthetic intermediate farnesyl pyrophosphate (25). *DPP1* is a member of a four-gene family in *C. albicans*, and deletion of the family member *DPP3* causes a reduction in farnesol accumulation (24). We expect that reduced *DPP1* gene expression in the mutant leads to decreased overall diacylglycerol pyrophosphate phosphatase activity, thus reducing farnesol production.

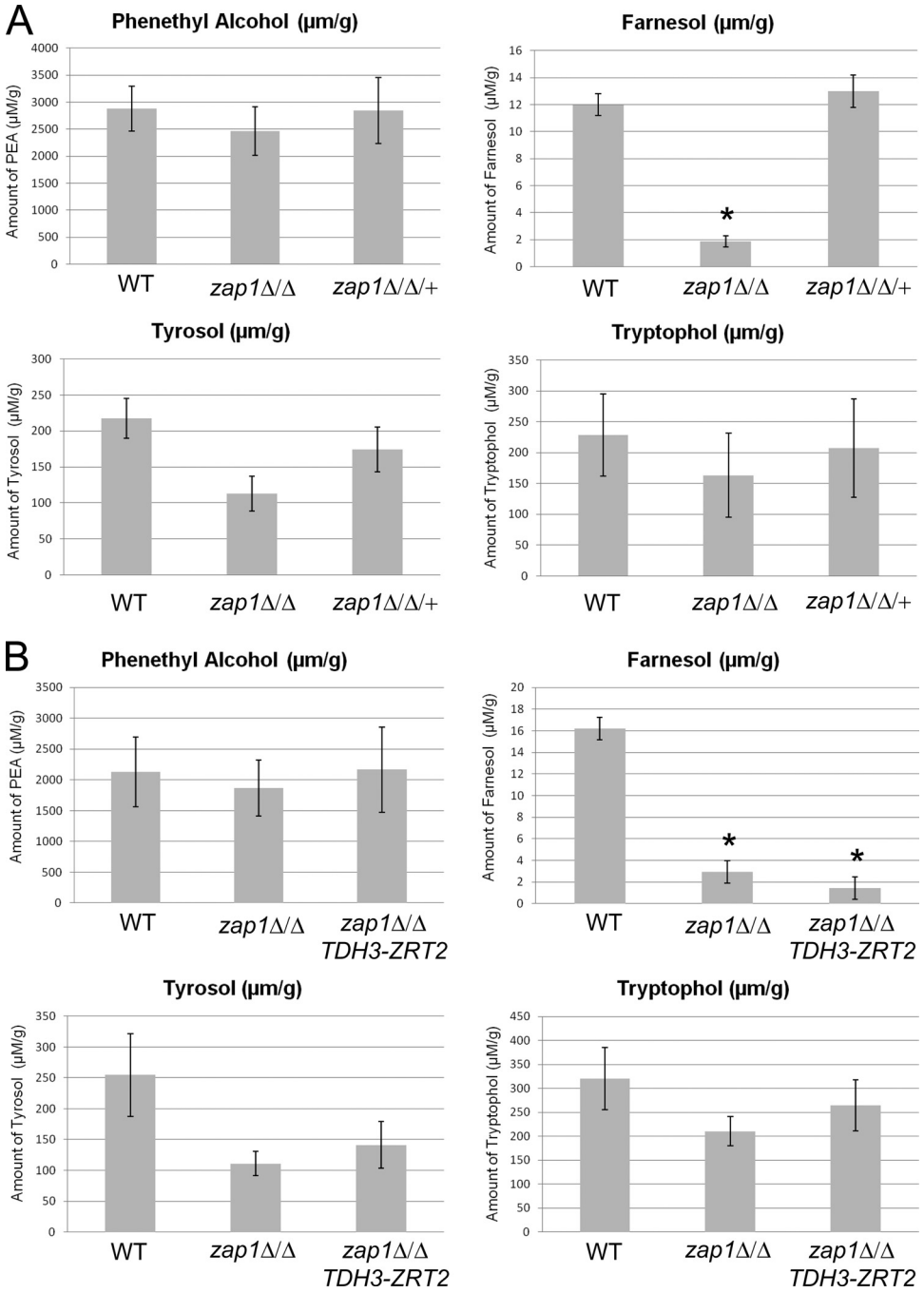

FIG. 4. Measurement of QS molecule accumulation in biofilms. (A) Supernatants from 48-h biofilms of the mutant strain CJN1201 (*zap1*Δ/Δ), the complemented strain CJN1193 (*zap1*Δ/Δ/+), and the reference wild-type strain DAY185 (*ZAP1*/*ZAP1*) were assayed for accumulation of phenethyl alcohol (PEA), farnesol, tyrosol, and tryptophol using GC-MS. The asterisk indicates that farnesol levels were significantly different from those of DAY185 in the *zap1*Δ/Δ mutant strain ($P = 0.0001$). (B) Supernatants from 48-h biofilms of the mutant strain CJN1201 (*zap1*Δ/Δ); the mutant strain overexpressing the zinc transporter gene *ZRT2*, CJN1655 (*TDH3-ZRT2* in *zap1*Δ/Δ); and the reference wild-type strain, DAY185 (*ZAP1*/*ZAP1*), were assayed as for panel A. The asterisks indicate that farnesol levels were significantly different from those of DAY185 in the *zap1*Δ/Δ mutant strain ($P = 0.0097$) and the *zap1*Δ/Δ *TDH3-ZRT2* strain ($P = 0.0061$). The error bars indicate standard deviations.

It seems counterintuitive that the *zap1*Δ/Δ mutant biofilm would accumulate excess yeast cells, given that it has low levels of farnesol. However, a similar paradox exists for the hyperfilamentous *tup1*Δ/Δ and *nrg1*Δ/Δ mutants (1). Specifically, we note that *tup1*Δ/Δ and *nrg1*Δ/Δ mutants grow almost exclusively as filamentous cells, yet they overproduce farnesol (21). The fact that cellular morphology does not always correlate with QS molecule production in mutant strains emphasizes the utility of our biosensor strain approach. The biosensor permits sampling of a biofilm environment independently of mutant cell morphology. Our re-

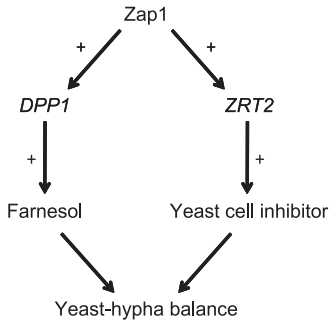

FIG. 5. Zap1 regulation of cell-cell signaling in biofilms. Zap1 has two roles that influence the yeast-hypha balance in biofilms through intercellular signaling. First, Zap1 promotes accumulation of farnesol, an inhibitor of hypha formation. We believe that this role of Zap1 is mediated through its control of *DPP1*, which specifies a putative diacylglycerol pyrophosphate phosphatase that may generate farnesol from farnesyl pyrophosphate (24). Second, Zap1 promotes accumulation of a postulated diffusible yeast cell inhibitor. We propose the existence of this molecule to explain the increased accumulation of yeast form cells in *zap1*Δ/Δ mutant biofilms. (A logically equivalent possibility is that Zap1 blocks accumulation of a postulated diffusible hypha inhibitor.) This function of Zap1 is mediated by its effects on the zinc uptake gene *ZRT2*.

sults suggest that a potentially significant mechanism of *C. albicans* cell-cell signaling has yet to be defined. A detailed comparison of the extracellular metabolome of wild-type, *zap1*Δ/Δ, and *zap1*Δ/Δ *TDH3-ZRT2* strains should define relevant candidate molecules. It will be interesting to determine whether the molecule's activity is manifested only in a low-farnesol environment.

How might Zap1 be related to the other transcription factors known to regulate farnesol production, Nrg1 and Tup1? Kebaara et al. have proposed that Nrg1 and Tup1 may act in a feedback circuit (21). Specifically, farnesol induces Tup1 RNA and protein, and that in turn represses filamentous growth and further production of farnesol. We can fit Zap1 into that model with the suggestion that Zap1 may be a negative regulator of Nrg1 or Tup1. As expected from the model, *NRG1* and *TUP1* RNAs are upregulated 1.3-fold in biofilms of the *zap1*Δ/Δ mutant compared to wild-type and complemented strains (unpublished results). Indeed, for the yeast *S. cerevisiae*, overexpression of *S. cerevisiae* Zap1 (ScZap1) reduces *ScTUP1* RNA levels, as expected if a negative Zap1-Tup1 relationship were evolutionarily conserved (6).

ACKNOWLEDGMENTS

This work was supported by NIH grant R01 AI067703 to A.P.M.

We acknowledge our late friend and colleague Mitchell E. Johnson for expert advice regarding the GC-MS analyses.

REFERENCES

1. **Biswas, S., P. Van Dijck, and A. Datta.** 2007. Environmental sensing and signal transduction pathways regulating morphopathogenic determinants of Candida albicans. Microbiol. Mol. Biol. Rev. **71:**348–376.
2. **Blankenship, J. R., S. Fanning, J. J. Hamaker, and A. P. Mitchell.** 2010. An extensive circuitry for cell wall regulation in Candida albicans. PLoS Pathog. **6:**e1000752.
3. **Brachmann, C. B., et al.** 1998. Designer deletion strains derived from Saccharomyces cerevisiae S288C: a useful set of strains and plasmids for PCR-mediated gene disruption and other applications. Yeast **14:**115–132.
4. **Chen, H., and G. R. Fink.** 2006. Feedback control of morphogenesis in fungi by aromatic alcohols. Genes Dev. **20:**1150–1161.
5. **Chen, H., M. Fujita, Q. Feng, J. Clardy, and G. R. Fink.** 2004. Tyrosol is a quorum-sensing molecule in Candida albicans. Proc. Natl. Acad. Sci. U. S. A. **101:**5048–5052.
6. **Chua, G., et al.** 2006. Identifying transcription factor functions and targets by phenotypic activation. Proc. Natl. Acad. Sci. U. S. A. **103:**12045–12050.
7. **Davis, D., J. E. Edwards, Jr., A. P. Mitchell, and A. S. Ibrahim.** 2000. Candida albicans RIM101 pH response pathway is required for host-pathogen interactions. Infect. Immun. **68:**5953–5959.
8. **Davis-Hanna, A., A. E. Piispanen, L. I. Stateva, and D. A. Hogan.** 2008. Farnesol and dodecanol effects on the Candida albicans Ras1-cAMP signalling pathway and the regulation of morphogenesis. Mol. Microbiol. **67:**47–62.
9. **Eide, D. J.** 2009. Homeostatic and adaptive responses to zinc deficiency in Saccharomyces cerevisiae. J. Biol. Chem. **284:**18565–18569.
10. **Finkel, J. S., and A. P. Mitchell.** 2011. Genetic control of Candida albicans biofilm development. Nat. Rev. Microbiol. **9:**109–118.
11. **Fux, C. A., J. W. Costerton, P. S. Stewart, and P. Stoodley.** 2005. Survival strategies of infectious biofilms. Trends Microbiol. **13:**34–40.
12. **Gerami-Nejad, M., K. Dulmage, and J. Berman.** 2009. Additional cassettes for epitope and fluorescent fusion proteins in Candida albicans. Yeast **26:**399–406.
13. **Ghosh, S., B. W. Kebaara, A. L. Atkin, and K. W. Nickerson.** 2008. Regulation of aromatic alcohol production in Candida albicans. Appl. Environ. Microbiol. **74:**7211–7218.
14. **Granger, B. L., M. L. Flenniken, D. A. Davis, A. P. Mitchell, and J. E. Cutler.** 2005. Yeast wall protein 1 of Candida albicans. Microbiology **151:**1631–1644.
15. **Hasan, F., I. Xess, X. Wang, N. Jain, and B. C. Fries.** 2009. Biofilm formation in clinical Candida isolates and its association with virulence. Microbes Infect. **11:**753–761.
16. **Hawser, S. P., and L. J. Douglas.** 1994. Biofilm formation by Candida species on the surface of catheter materials in vitro. Infect. Immun. **62:**915–921.
17. **Heilmann, C. J., et al.** 2011. Hyphal induction in the human fungal pathogen Candida albicans reveals a characteristic wall protein profile. Microbiology **157:**2297–2307.
18. **Hogan, D. A.** 2006. Talking to themselves: autoregulation and quorum sensing in fungi. Eukaryot. Cell **5:**613–619.
19. **Hogan, D. A., A. Vik, and R. Kolter.** 2004. A Pseudomonas aeruginosa quorum-sensing molecule influences Candida albicans morphology. Mol. Microbiol. **54:**1212–1223.
20. **Hornby, J. M., et al.** 2001. Quorum sensing in the dimorphic fungus Candida albicans is mediated by farnesol. Appl. Environ. Microbiol. **67:**2982–2992.
21. **Kebaara, B. W., et al.** 2008. Candida albicans Tup1 is involved in farnesol-mediated inhibition of filamentous-growth induction. Eukaryot. Cell **7:**980–987.
22. **Kim, M. J., M. Kil, J. H. Jung, and J. Kim.** 2008. Roles of zinc-responsive transcription factor Csr1 in filamentous growth of the pathogenic yeast Candida albicans. J. Microbiol. Biotechnol. **18:**242–247.
23. **Martins, M., et al.** 2007. Morphogenesis control in Candida albicans and Candida dubliniensis through signaling molecules produced by planktonic and biofilm cells. Eukaryot. Cell **6:**2429–2436.
24. **Navarathna, D. H., et al.** 2007. Effect of farnesol on a mouse model of systemic candidiasis, determined by use of a DPP3 knockout mutant of Candida albicans. Infect. Immun. **75:**1609–1618.
25. **Nickerson, K. W., A. L. Atkin, and J. M. Hornby.** 2006. Quorum sensing in dimorphic fungi: farnesol and beyond. Appl. Environ. Microbiol. **72:**3805–3813.
26. **Nobile, C. J., and A. P. Mitchell.** 2005. Regulation of cell-surface genes and biofilm formation by the C. albicans transcription factor Bcr1p. Curr. Biol. **15:**1150–1155.
27. **Nobile, C. J., et al.** 2009. Biofilm matrix regulation by Candida albicans Zap1. PLoS Biol. **7:**e1000133.
28. **Ramage, G., S. P. Saville, B. L. Wickes, and J. L. Lopez-Ribot.** 2002. Inhibition of Candida albicans biofilm formation by farnesol, a quorum-sensing molecule. Appl. Environ. Microbiol. **68:**5459–5463.
29. **Sohn, K., C. Urban, H. Brunner, and S. Rupp.** 2003. EFG1 is a major regulator of cell wall dynamics in Candida albicans as revealed by DNA microarrays. Mol. Microbiol. **47:**89–102.
30. **Spreghini, E., D. A. Davis, R. Subaran, M. Kim, and A. P. Mitchell.** 2003. Roles of Candida albicans Dfg5p and Dcw1p cell surface proteins in growth and hypha formation. Eukaryot. Cell **2:**746–755.
31. **Staab, J. F., and P. Sundstrom.** 1998. Genetic organization and sequence analysis of the hypha-specific cell wall protein gene HWP1 of Candida albicans. Yeast **14:**681–686.
32. **Uppuluri, P., et al.** 2010. Dispersion as an important step in the Candida albicans biofilm developmental cycle. PLoS Pathog. **6:**e1000828.
33. **Wilson, R. B., D. Davis, and A. P. Mitchell.** 1999. Rapid hypothesis testing with Candida albicans through gene disruption with short homology regions. J. Bacteriol. **181:**1868–1874.
34. **Zhao, H., and D. J. Eide.** 1997. Zap1p, a metalloregulatory protein involved in zinc-responsive transcriptional regulation in Saccharomyces cerevisiae. Mol. Cell. Biol. **17:**5044–5052.